

Supporting Information for:

**Reactivity of Substituted Benzotrichlorides Toward Granular Iron,
Cr(II) and an Iron(II) Porphyrin: A Correlation Analysis**

Tamar Kohn, William A. Arnold and A. Lynn Roberts

Environmental Science and Technology

Supporting Information describes experimental details pertaining to the kinetic experiments and preparation of reductants; characterization of the FeTCP reductant (including determination of its half wave potential and the reduced Fe(II)TCP concentration); our investigation of electron transfer in reduction of BTC by Cr(II); typical time courses illustrating product development; computation of bond dissociation energies (BDE values); the derivation of rate expressions; and data pertaining to reactions with other R-CCl₃ compounds.

Experimental Details for Kinetic Experiments

Reduction by Cr(II): Stock solutions of Cr(II) were prepared by a procedure modified from ref. 1. Within a glove box (95% N₂/5% H₂ atmosphere), 0.5 M Cr(III) sulfate in deaerated 5 mM H₂SO₄ was placed in a polypropylene flask containing 50 g zinc powder, and the solution was stirred overnight. Once the Cr(III) had been reduced to Cr(II), the solution displayed a characteristic blue color. The Cr(II) solution was passed through a 0.25 μm filter to remove the Zn powder, and was subsequently stored in the glove box. Control experiments in the absence of Cr(II) failed to reveal any BTC degradation attributable to zinc colloids that might have been present.

Kinetic experiments were conducted at Cr(II) concentrations of 2.5 mM prepared by diluting the 0.5 M Cr(II) stock with appropriate amounts of acetonitrile and 5 mM H₂SO₄. The exact Cr(II) concentrations were determined before every experiment by UV/vis spectroscopy (Shimadzu UV-1601), using the molar extinction coefficient $\epsilon = 5.6 \text{ M}^{-1} \text{ cm}^{-1}$ at 714 nm (2).

Within the glove box, 20 mL aliquots of the Cr(II) solutions were added to 25 mL serum vials and were spiked with 40 μL of the stock solution of the BTC compound of interest to an initial concentration of 40 μM. Samples (1 mL) were removed at regular intervals through glass tuberculin syringes equipped with Teflon needles. The samples were immediately extracted into 10 mL of hexane by shaking for 1 minute. Extraction efficiencies were approximately 100 %, except for BA, for which it was 33 %. For product analysis, selected 2-mL samples of the solution phase were extracted into 1 mL of hexane as well as into 1 mL of ethyl acetate (for the detection of benzyl alcohol). If necessary, extracts were further diluted with the appropriate solvent prior to analysis. Reactions were performed in duplicate or triplicate with good reproducibility.

Reduction by Fe(II)TCP: A solution of 25 μM Fe(III)TCP was prepared inside the glove

box in a 50:50 (v/v) solution of acetonitrile and deaerated, deionized (DI) water at pH 11 (adjusted by adding NaOH). Neither iron nor zinc powder successfully reduced Fe(III)TCP; palladized iron was, therefore, used as a reductant.

Palladized iron was prepared by adding 5 g of acid-washed electrolytic iron powder to a solution prepared from 120 mg K_2PdCl_6 (98 %, Aldrich) in 200 mL deaerated 0.01 M HCl. The solution was stirred until all its orange color had disappeared, indicating that the palladium had been plated onto the iron. The iron powder was then rinsed three times with water and dried in the oven at 100°C under a constant flow of N_2 .

Portions (5g) of palladized iron were transferred to 160 mL serum vials, and 100 mL of the dark green Fe(III)TCP solution was added. The vials were sealed with a Teflon septum, were wrapped in aluminum foil, and were placed on a roller table outside the glovebox. After 2 days of mixing, the solution turned red, indicating partial reduction of Fe(III)TCP to Fe(II)TCP. The reduced solution and the palladized iron were separated by drawing the iron to the bottom of the serum vial with a magnetic stir plate and removing the solution from the top of the vial. Control experiments in the absence of FeTCP showed no measurable degradation of BTC that might stem from incomplete separation of palladized iron according to this procedure.

Experiments were conducted within the glovebox, using a solution with an actual reduced Fe(II)TCP concentration of 6.4 μ M (and a Fe(III)TCP concentration of 18.6 μ M). The concentration of Fe(II)TCP was estimated by UV/vis measurements at 330 nm, as described in the following section.

Aliquots (20 mL) of the reduced FeTCP solution in 25 mL serum vials were spiked with 20 μ L of the stock solution of the BTC compound of interest to an initial concentration of 1 μ M. Samples (2 mL) were taken using a glass tuberculin syringe with a Teflon needle, and were extracted into 1 mL of hexane. Despite the low initial reductant concentration, initial data closely

approximated exponential decay. All kinetic experiments were repeated with a second batch of Fe(II)TCP solution (data not shown), with good reproducibility of the relative rate constants. For product determination, experiments were conducted at an approximate initial Fe(II)TCP concentration of 250 μM and an initial BTC concentration of 10 μM . After four half lives, a 5-mL sample aliquot was extracted with 1 mL ethyl acetate, and a second 1-mL aliquot with 1 mL of hexane.

Reduction by Granular Iron: Reactions with granular iron were carried out in headspace-free 160 mL serum vials, using electrolytic iron powder that had been acid washed according to ref. 3. Inside the glove box, the vials were filled with 250 mg of iron powder and a deaerated solution of 50:50 (v/v) acetonitrile and aqueous buffer (50 mM Tris buffer and 0.1 M NaCl at pH 7.2), and were sealed with Teflon septa and a crimp seal. The vials were removed from the glove box and were placed on a roller table overnight. The following day the vials were spiked with the stock solution of the BTC compound of interest to an initial concentration of 40 μM . Samples were removed at intervals through a glass tuberculin syringe. A 1-mL aliquot of a deaerated 50:50 acetonitrile : buffer solution was injected simultaneously into the vial to replace the volume withdrawn. Samples were extracted as described for the Cr(II) system. Reactions were performed in triplicate with good reproducibility.

Characterization of FeTCP Solutions

The concentration of Fe(II)TCP was estimated by UV/vis spectroscopy. The spectrum of Fe(III)TCP in water shows a peak at 330 nm, which decreases upon reduction to Fe(II)TCP. In an airtight cuvette, the absorbance (Abs) at 330 nm of the reduced reaction solution was measured. The Fe(II)TCP solution was subsequently oxidized by air, and Abs (330 nm) of the oxidized solution was determined. The increase in Abs (330 nm) between the reduced and the

oxidized solution can be attributed to the oxidation of Fe(II)TCP and is therefore a measure of the initial concentration of Fe(II)TCP in the reduced reaction solution. The molar extinction coefficient ϵ (330 nm) for Fe(III)TCP was estimated by dividing Abs (330 nm) of the oxidized solution by the nominal total FeTCP concentration, obtained gravimetrically. This ignores any potential losses of FeTCP through sorption to the palladized iron used to reduce it.

The half-wave potential ($E_{1/2}$) of FeTCP in water was measured by cyclic voltammetry using a BAS CV-50W instrument (Bioanalytical Systems, Inc.) equipped with a glassy carbon working electrode, an Ag/AgCl (sat. KCl) reference electrode, and platinum mesh as the counter electrode. The solution contained 2 mM FeTCP and 50 mM NaCl in water. Even though the solution was continuously sparged with high-purity nitrogen, the oxidizing current was difficult to measure, presumably as a result of Fe(II)TCP oxidation by adventitious dissolved oxygen in solution. Our measured $E_{1/2}$ value should therefore be considered an approximation only.

Capillary Electrophoretic Studies of CrCl^{2+} Resulting from Reduction of Benzotrichloride by Cr(II)

To assess whether $\text{Cr}(\text{H}_2\text{O})_6^{2+}$ reacts with benzotrichloride (BTC) via an inner or an outer sphere mechanism, we used capillary electrophoresis to investigate the chromium complexes present before and after reaction with BTC, according to a method described in ref. 4. Analysis was performed using a 20 mM phosphoric acid buffer (H_3PO_4 , > 99 %, Aldrich) at pH 2, using a Beckman P/ACE MDQ capillary electrophoresis instrument equipped with a diode array detector. The injection time was 10 s, and the separation was performed at an applied voltage of 30 kV. Sample detection was performed at wavelengths of 200 nm, 214 nm and 254 nm. Retention times were determined using standard solutions prepared from chromium(III) nitrate

($\text{Cr}(\text{NO}_3)_3 \cdot 9 \text{H}_2\text{O}$, 99 %, Aldrich) for $\text{Cr}(\text{H}_2\text{O})_6^{3+}$, and from chromium(III) chloride ($\text{CrCl}_3 \cdot 6 \text{H}_2\text{O}$, J.T. Baker) for CrCl^{2+} and CrCl_2^+ .

Good separation of $\text{Cr}(\text{H}_2\text{O})_6^{3+}$, CrCl^{2+} and CrCl_2^+ could be obtained in standard solutions (Fig. S1(a)). To avoid overwhelming interference by excess chromium species, 200 μM Cr(II) was reacted with 200 μM of BTC (in the absence of acetonitrile). The solution was analyzed by CE within 30 minutes of reaction.

Figure S1a shows the electropherogram of a standard solution containing the two chloro-complexes, of the reacted solution, and of a 200 μM Cr(II) blank solution allowed to oxidize in air. When comparing the electropherograms of the reacted and the unreacted solutions at 214 nm, a large peak (indicative of CrCl^{2+}) is evident in the reacted solution. This confirms that reduction of BTC by Cr(II) occurs by inner sphere electron transfer.

Another characteristic feature of the reacted solution is a peak eluting at about 2.8 minutes. This peak can also be seen in the electropherogram obtained at 254 nm (Fig. S1(b)). Because inorganic chromium complexes show very little absorbance at this wavelength, this peak may reflect a charged aromatic species. We tentatively attribute this peak to a chromium-associated product as described by Anet (5) and by Kochi and Davis (6). Based on its electromigration time, we speculate that the product is $[\text{C}_6\text{H}_5\text{CCl}_2\text{-Cr}(\text{H}_2\text{O})_5]^{2+}$. Its hydrodynamic radius is expected to be greater than that of CrCl^{2+} , because a chlorine ligand has been replaced by a larger aromatic ligand. It should therefore migrate more slowly than CrCl^{2+} , but more rapidly than CrCl_2^+ , consistent with the observed electropherogram (Fig. S1(a)). This product is not detectable by GC/MS, and may account for the missing mass in our system. It is not likely that other charged reaction products are present in our solution, because protonation of BA (7) as well as the hydration and deprotonation of BA (8) are negligible at a solution pH of 2.5.

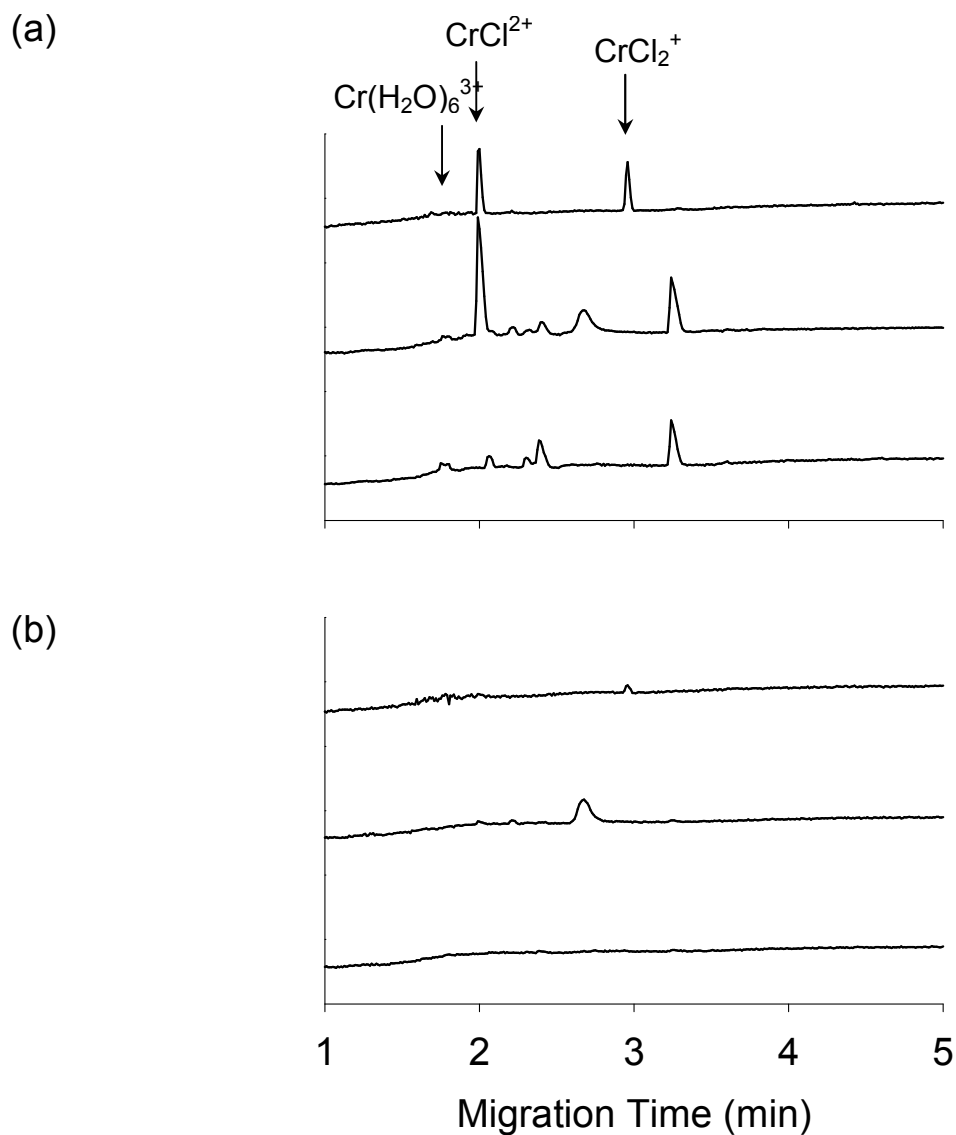


Figure S1: (a) Electropherograms obtained at 214 nm. Top: standard solution of $\text{CrCl}(\text{5H}_2\text{O})^{2+}$ and $\text{CrCl}_2(\text{4H}_2\text{O})^+$. Middle: chromium sulfate solution reduced by $\text{Zn}(0)$ and reacted with BTC. Bottom: chromium sulfate reduced by $\text{Zn}(0)$ and re-oxidized by air. Peaks at 3.2 minutes may represent a Cr(III) sulfate species. (b): The same electropherograms obtained at 254 nm. The peak at 2.8 minutes in the middle electropherogram may represent a Cr-associated aromatic product.

Time Courses and Reaction Products

Typical time courses and pseudo-first-order model fits are shown in Fig. S2. A scheme illustrating the proposed reaction pathways is provided as Fig. 1 in the main text.

Cr(II): Although most experiments were conducted at a Cr(II) concentration of 2.5 mM (and a substituted BTC concentration of 40 μ M), additional experiments were conducted at Cr(II) concentrations varying from 1 to 25 mM. Reactions of Cr(II) with BTC proved first order with respect to the Cr(II) concentration, as shown by a slope of 1.09 (\pm 0.27) in plotting the logarithm of pseudo-first-order rate constants for BTC decay as a function of the logarithm of the Cr(II) concentration (data not shown).

The reaction of Cr(II) with BTC is thought to proceed by the scheme shown in Fig. 1(a). The initial step is a dissociative electron transfer, followed by a second electron transfer and halide ion elimination to form a chlorophenyl carbene (or carbenoid) species. This species can react via insertion of the carbene into an H-OH bond to yield BA, or it can undergo further reduction to benzyl alcohol via a phenyl carbenoid intermediate. Benzyl alcohol could in principle also stem from BA reduction (9), although control experiments indicated that this reaction occurred at negligible rates under the conditions of this study.

FeTCP: The reduction of BTC by FeTCP resulted in coupling products. Wade and coworkers (10,11) report the formation of both hydrogenolysis and coupling products from the reduction of alkyl polyhalides by an FeP (deuterohemin IX). We did not observe the hydrogenolysis product BC. Because samples for product analysis were only taken after four half lives of the reaction, however, we cannot preclude the existence of BC as a reaction intermediate. The proposed reaction scheme is shown in Fig. 1(b).

Granular iron: A plot of initial BTC concentration vs. initial rate of reaction is roughly linear over the range of initial BTC concentrations from 5 to 300 μ M (data not shown). This

implies extensive competition for reactive surface sites does not exist under our experimental conditions. A linear dependence of initial rate on initial concentration either indicates adsorption-limited reaction kinetics, or surface-reaction limited kinetics at BTC concentrations less than the equilibrium constant for sorption to the reactive surface sites (12).

This process would be initiated by a dissociative one-electron transfer, as illustrated in Fig. 1(c). The resulting radical species could then either undergo further reduction and proton transfer to BC, or it could couple with another radical. BC reacted only slowly with granular iron (data not shown). Toluene is thus not formed by stepwise dehalogenation, but rather by way of carbenoid intermediates and proton transfer steps, analogous to the formation of ethane from 1,1,1-TCA (3).

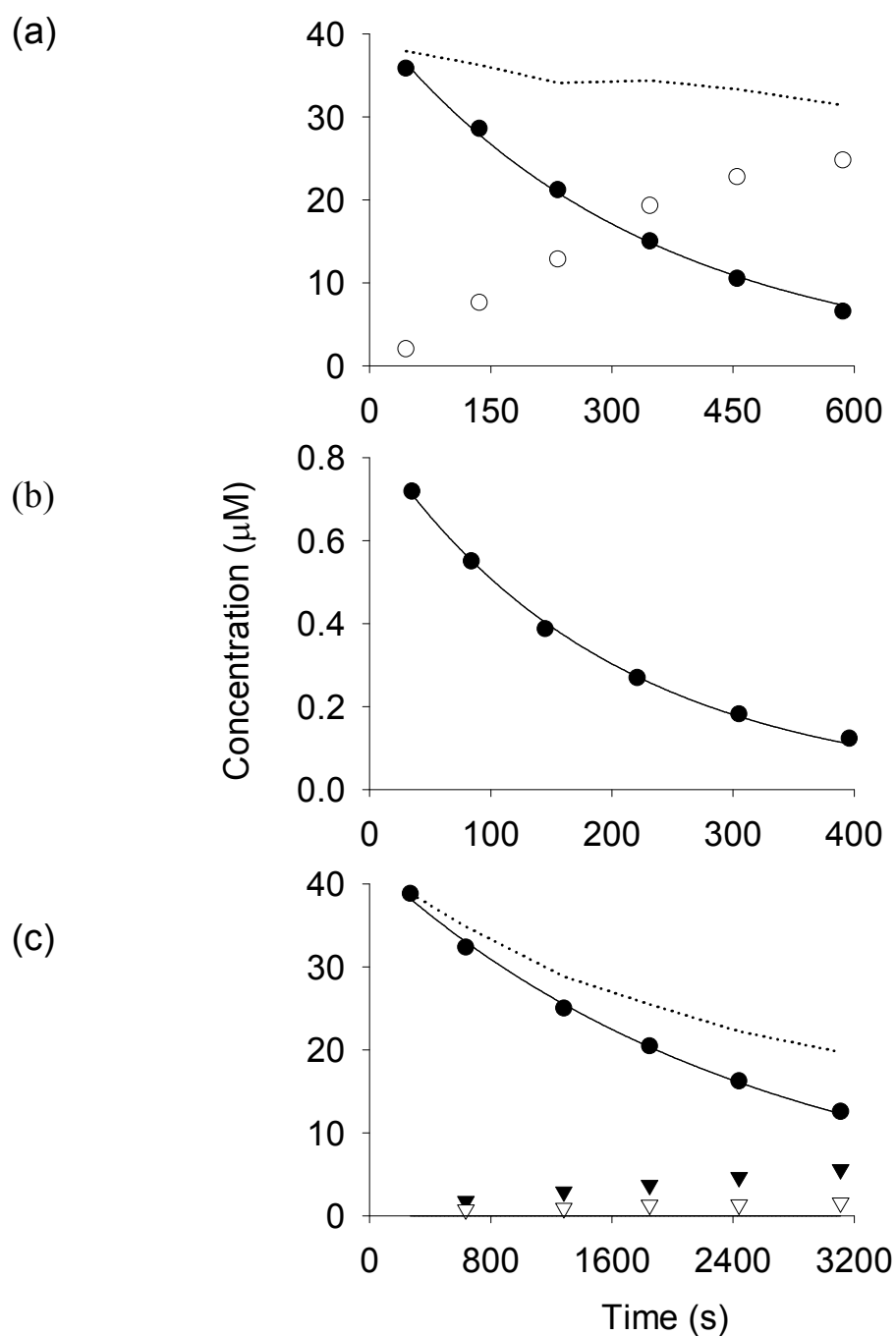


Figure S2: Typical time courses for reaction of BTC with **(a)** $2.5 \text{ mM Cr}(\text{H}_2\text{O})_6^{2+}$, **(b)** $6.4 \mu\text{M Fe(II)TCP}$, and **(c)** $250 \text{ mg Fe(0) per 160 mL}$ of solution, showing accumulation of quantifiable products. The solid lines indicate model fits to exponential decay. All reactions were conducted in 50:50 (v/v) aqueous solution/acetonitrile. Symbols indicate BTC (\bullet), BA (\circ), BC (\blacktriangledown), toluene (∇), and carbon mass balance (\cdots). Products that were not quantified but that were observed include benzyl alcohol (Cr system, trace amounts only) and coupling products (observed in both the Fe(II)TCP and Fe(0) systems).

Computation of Bond Dissociation Energies (BDEs)

BDEs were calculated for the reaction $RX \rightarrow R\cdot + X\cdot$. Assuming ideal gas behavior for a rigid rotor with all vibrations treated as harmonic oscillators and the electronic partition function equal to the ground-state degeneracy, the absolute gas-phase free energy for a molecule is computed as the sum of the Born-Oppenheimer electronic ground-state energy (including nuclear repulsion energy), zero-point vibrational energy, and translational, rotational, vibrational, and electronic thermal contributions (13). All molecular geometries were optimized at the density functional level of theory. The functional employed was Becke's (14,15) 3-parameter exchange-correlation operator which combines exact Hartree-Fock exchange (13) with Slater's (16) local exchange functional and Becke's (17) 1988 gradient correction to Slater's functional, and for correlation employs the gradient corrected correlation functional of Lee, Yang, and Parr (18). This combination is denoted B3LYP (19). To verify the nature of all minima and to calculate the sum of electronic and thermal enthalpies at 298 K, analytic frequency calculations were also performed using the B3LYP functional. All calculations employed the 6-311G (20,21) basis set supplemented by diffuse functions (2 sets of d functions and one set of f functions on heavy atoms, and 1 set of p functions on hydrogen; 6-311+G(2df,p)) (22,23). All calculations were carried out with the Gaussian 03 electronic structure program suite (24). BDEs were computed from the appropriate calculated enthalpies for the parent molecule and resultant radical species.

The scatter plots of reaction rate constants for reduction of substituted BTCs in all three systems against bond dissociation energies are shown in Fig. S3.

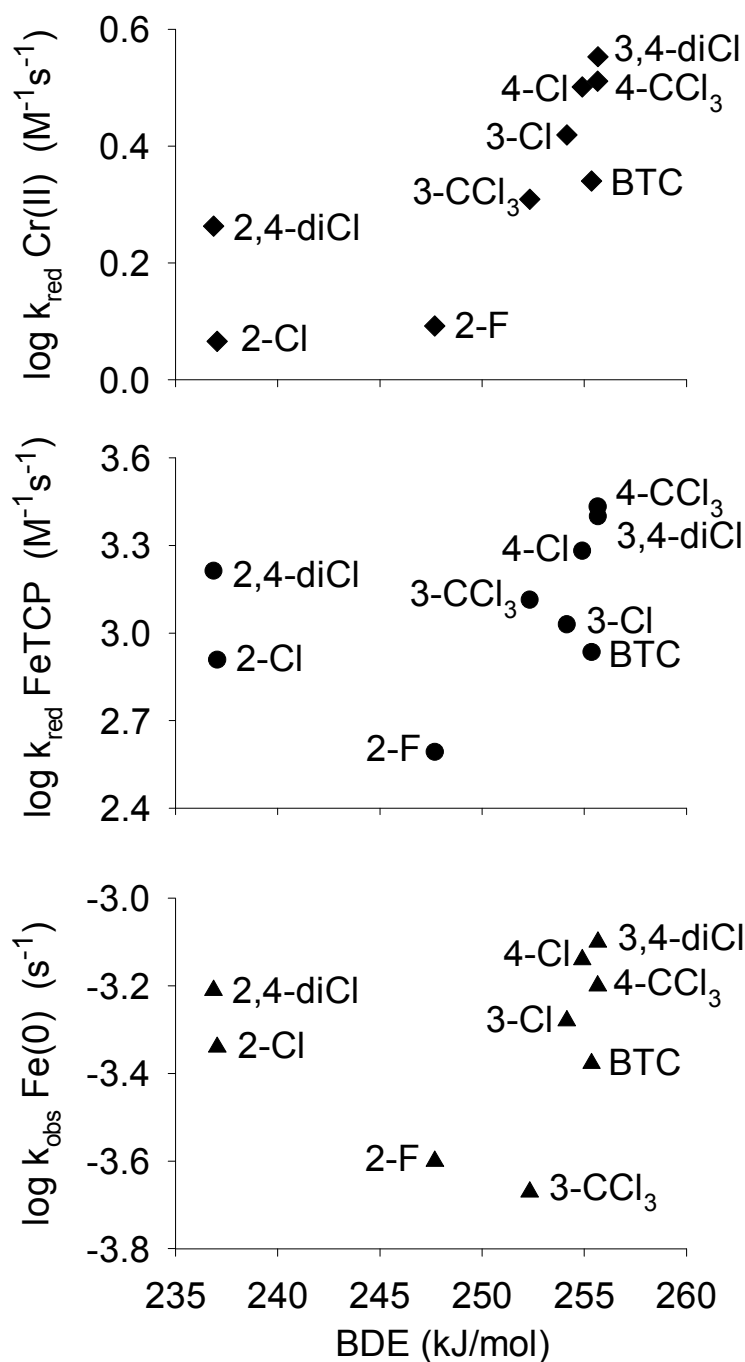


Figure S3: Scatter plots of reaction rate constants for reduction of substituted BTCs in all three systems against bond dissociation energies for the reaction $\text{RX} \rightarrow \text{R} + \text{X}$. Note that hexachloro-m-xylene (3-CCl₃) and hexachloro-p-xylene (4-CCl₃) have two identical reaction centers. The corresponding rate constants were therefore divided by a statistical factor of two for the purposes of these plots.

Derivation of Rate Expressions

Consider an example of a simple elementary bimolecular reaction (e.g., an S_N2 reaction):



The rate of reaction can be expressed as:

$$\text{rate} = -k[A][B] \quad (\text{S2})$$

where k is a second-order rate constant. According to transition state theory, k is related to the activation energy ΔG^\ddagger as follows:

$$k = \frac{kT}{h} \cdot e^{-\frac{\Delta G^\ddagger}{RT}} = c \cdot e^{-\frac{\Delta G^\ddagger}{RT}} \quad (\text{S3})$$

The pre-exponential factor is composed of the absolute temperature T, the Boltzmann constant **k** ($1.38 \times 10^{-23} \text{ J} \cdot \text{K}^{-1}$), and the Planck constant h ($6.63 \times 10^{-34} \text{ J} \cdot \text{s}$), and can be expressed as a constant c if all reactions under consideration are conducted at a single temperature.

To compare the rate constants obtained in two different systems, the logarithm of the rate constants in two systems can be correlated against one another. Consider the case where two systems, 1 and 2, are allowed to react with a common group of reactants. For each rate constant $k_1(i)$ in system 1 we can write:

$$\log k_1(i) = \log c - \frac{\Delta G_1^\ddagger(i)}{2.303RT} \quad (\text{S4})$$

and for system 2:

$$\log k_2(i) = \log c - \frac{\Delta G_2^\ddagger(i)}{2.303RT} \quad (\text{S5})$$

The slope b from a correlation of $\log k_1$ against $\log k_2$ can be expressed as:

$$b = \frac{d \log k_1}{d \log k_2} = \frac{\Delta \log k_1}{\Delta \log k_2} \quad (\text{S6})$$

Using Equations S4 and S5, we can write for $\Delta \log k_1$ and $\Delta \log k_2$

$$\Delta \log k_1 = \log c - \frac{\Delta G_1^\ddagger(ii)}{2.303RT} - \log c + \frac{\Delta G_1^\ddagger(i)}{2.303RT} = \frac{\Delta \Delta G_1^\ddagger}{2.303RT} \quad (\text{S7})$$

and

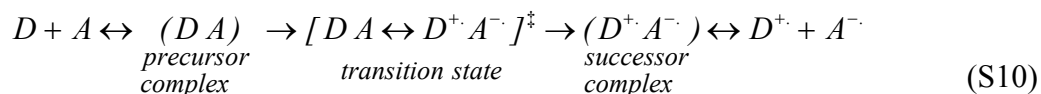
$$\Delta \log k_2 = \log c - \frac{\Delta G_2^\ddagger(ii)}{2.303RT} - \log c + \frac{\Delta G_2^\ddagger(i)}{2.303RT} = \frac{\Delta \Delta G_2^\ddagger}{2.303RT} \quad (\text{S8})$$

where $\Delta G_1^\ddagger(i)$ and $\Delta G_1^\ddagger(ii)$ reflect the activation energies for the reactions in system 1 with species i and ii, and $\Delta G_2^\ddagger(i)$ and $\Delta G_2^\ddagger(ii)$ are the activation energies for reactions with the same species in system 2. Substituting Eqs. S7 and S8 into the expression for b (Eq. S6), we find:

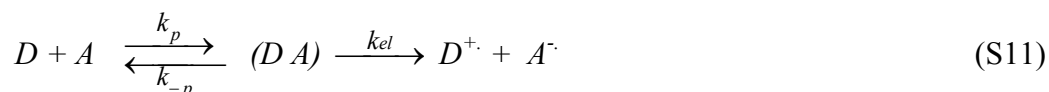
$$b = \frac{\Delta \Delta G_1^\ddagger}{\Delta \Delta G_2^\ddagger} = \frac{\Delta \Delta H_1^\ddagger - \Delta \Delta S_1^\ddagger T}{\Delta \Delta H_2^\ddagger - \Delta \Delta S_2^\ddagger T} \quad (\text{S9})$$

The slope b of the correlation thus reflects the relative sensitivity of the activation barriers in each system to changes in structure of the common reactants in question. If the slope is unity, both systems are identically sensitive to changes in structure of the common reactants. If the slope differs from unity, one system is more affected by structural changes. Such differences need not stem from different reaction mechanisms, but could originate from varying contributions of the enthalpic (ΔH^\ddagger) and entropic (ΔS^\ddagger) terms (Eq. S9).

A somewhat more complex situation is encountered when reactions occur by a one-electron transfer between an electron donor D and an electron acceptor A in homogeneous solution. Such reactions can be envisioned as occurring through a sequence of steps involving the creation of a precursor complex, the actual electron transfer, the formation of a successor complex and finally the separation into products (25):



Probable rate-limiting steps in this sequence are precursor formation, or else electron transfer in the transition state. The simplest way of deriving a rate expression that accounts for both of these processes is to formulate the precursor formation as a reversible process, followed by an irreversible electron transfer step (25):



The equilibrium constant for the precursor formation can be expressed as $K_p = k_p/k_{-p}$. The rate of electron transfer can be written as:

$$rate = -k_{el}[DA] \quad (\text{S12})$$

A steady-state approximation for the precursor complex (DA) and substitution into Eq. S12 yields the overall rate:

$$rate = \frac{-k_p}{1 + \frac{k_p}{K_p k_{el}}} [D][A] \quad (\text{S13})$$

If $\frac{k_p}{K_p k_{el}} \gg 1$, then the rate expression can be simplified as:

$$rate = -K_p k_{el}[D][A] = -\frac{k_p}{k_{-p}} k_{el}[D][A] = -k' [D][A] \quad (\text{S14})$$

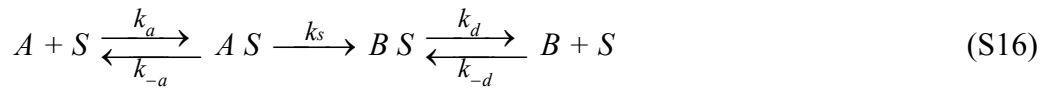
in which k' represents a composite rate constant equal to $K_p k_{el}$. In this case, a slope of a $\log k_1$ vs. $\log k_2$ plot that differs from unity could arise from two causes. Either the susceptibility of ΔG^\ddagger to changes in the substrates differs for k_{el} in each system, or else the equilibrium constants corresponding to the formation of the precursor complex (K_p values) differ in magnitude.

If $\frac{k_p}{K_p k_{el}} \ll 1$, the rate expression becomes:

$$rate = -k_p [D][A] \quad (\text{S15})$$

As for the case of an S_N2 reaction, the rate constant (k_p) reflects an elementary process and is not a composite rate constant. A slope of a $\log k_1$ vs. $\log k_2$ plot different from unity indicates that the ΔG^\ddagger values of the two systems vary to a different extent upon changes in the substrate, potentially because of differences in enthalpic or entropic barriers to the reaction.

Rate constants in heterogeneous systems also tend to represent composite rather than elementary rate constants. A good model for the description of reactions in heterogeneous systems is the Langmuir-Hinshelwood-Hougen-Watson (LHHW) approach (ref. 12 and references therein). This model incorporates three potentially rate-limiting steps. The first step is a Langmuir-type adsorption of the parent compound to a reactive site on the surface. In the second step, the parent compound undergoes reaction at the surface, and the third step corresponds to desorption of the product from the surface:



A is the substrate, S is a vacant active site on the iron, B is the product, k_a and k_{-a} are the adsorption and desorption rate constants for the substrate, k_s is the reaction rate constant for the surface reaction, and k_d and k_{-d} are the adsorption and desorption rate constants for the product. The equilibrium constants for adsorption and desorption of parent compound and product can be defined as $K_A = k_a/k_{-a}$ and $K_B = k_d/k_{-d}$. The total number of sites can be expressed as:

$$S_{tot} = S + AS + BS \quad (\text{S17})$$

AS and BS are sites occupied by the substrate A or the product B.

If adsorption to the iron is the rate-limiting step, surface reaction and product desorption are relatively fast such that neither S_A nor S_B accumulate. The overall rate can then be simply expressed as:

$$rate = -k_a [A][S] \quad (\text{S18})$$

In this case k_a once again represents an elementary rate constant. Its magnitude reflects the molecular properties facilitating adsorption, such as electron donor-acceptor interactions. As was discussed above for elementary reactions, a slope of a $\log k_1$ vs. $\log k_2$ plot that is different from unity indicates that the ΔG^\ddagger values of these two systems differ in their response to changes in the structure of the common reagent.

Alternatively, if the rate-limiting step were the surface reaction, the reaction rate can be expressed as:

$$rate = -k_s [AS] \quad (S19)$$

Assuming adsorption and desorption equilibrium for the contaminant A and a fast desorption of the product B, we can write for the occupied sites AS and BS

$$[AS] = K_A [A][S] \quad (S20)$$

$$[BS] = K_B^{-1} [B][S] \approx 0 \quad (S21)$$

Substituting Eq. S20 into Eq.S19, and expressing the number of vacant sites S in terms of Eq. S17, we find the following expression for the overall rate:

$$rate = \frac{-k_s S_t K_A [A]}{1 + K_A [A]} \quad (S22)$$

If $K_A [A] \ll 1$, the rate can be expressed as

$$rate = -k_s S_t K_A [A] = -k_s S_t \frac{k_a}{k_{-a}} [A] = -k' S_t [A] \quad (S23)$$

where k' is a composite rate constant consisting of the surface-reaction rate constant k_s and the adsorption equilibrium constant K_A . This situation would be difficult to distinguish experimentally from an adsorption-limited reaction (Eq. S18). As with the case of electron transfer in homogeneous systems, a slope other than unity in a plot of $\log k_1$ vs. $\log k_2$ can either result from disparities in the susceptibility of ΔG^\ddagger to changes in the substrate, or from differences in the adsorption equilibrium constants. It can be expected that both enthalpic and entropic

factors contribute to the differences in ΔG^\ddagger values in reactions on surfaces. Variations in $\Delta\Delta G^\ddagger$ may reflect structural differences in reactive sites such as Fe(II). For example, Fe(II) adsorbed onto goethite may be more accessible for reaction with a contaminant than structural Fe(II) embedded in the crystal lattice of clay minerals such as reduced nontronite ($\text{Na}_{0.3}\text{Fe}_2^{3+}(\text{Si}, \text{Al})_4\text{O}_{10}(\text{OH})_2 \cdot n(\text{H}_2\text{O})$). K_A , which reflects the equilibrium constant for the adsorption of the substrate to the reactive site, can be expected to vary between different heterogeneous systems if the reactive sites are not identical. In a cross-correlation involving at least one heterogeneous system, a slope of unity might even be anticipated to be the exceptional result of coincidence rather than the rule.

In the situation where $K_A [A] \gg 1$, the rate simplifies to:

$$\text{rate} = -k_s S_t \quad (\text{S24})$$

In this case, the reaction rate would be independent of the contaminant concentration [A].

Reactions of organohalides in heterogeneous systems using granular iron as the reductant have been shown to be either adsorption or surface reaction limited (12). The case of a desorption limited reaction is therefore not considered further.

Reactions with Other R-CCl₃ Compounds

In addition to varying the substituents on the aromatic ring, the effect of substituents directly attached to the CCl₃ group were explored. Chloroform (CHCl₃, 99.9 %, Aldrich), fluorotrichloromethane (CCl₃F, 99+ %, Aldrich), 1,1,1-trichloroethane (1,1,1-TCA, 99.5 %, Aldrich) and 1,1,1,2-tetrachloroethane (1,1,1,2-TeCA, 99 %, Aldrich) were reacted with granular iron in Tris buffer at pH 7.2, in the absence of acetonitrile. Reactions were performed in an analogous manner to the BTC compounds, but the initial alkyl halide concentration was set to 100 μM using a methanolic spiking solution. Aliquots (1 mL) containing halogenated methanes were extracted with hexane. 1,1,1-TCA and 1,1,1,2-TeCA were not extracted with an organic solvent; rather, aqueous samples (1 mL) were transferred into 2.5 mL autosampler vials and stored in the freezer until analysis. The halogenated ethanes were analyzed by headspace GC using the system described in ref. 3, using a GS-Q PLOT column (30 m × 0.53 mm i.d., × 40 μm film thickness, Agilent Technologies) and flame ionization detection (FID). Headspace samples (200 μL) were injected in splitless mode, and the system was calibrated using the headspace of aqueous standards. The halogenated methanes were analyzed by GC/ECD as described in the accompanying article.

Rate constants for reaction with granular iron were cross-correlated to those determined for reaction with Cr(II) by Totten (26) in 5 mM H₂SO₄. The rate constants obtained in these experiments are shown in Table S1, along with pertinent molecular descriptors. Figure 3 in the main text shows the cross-correlation obtained for BTC and the four alkyl halides investigated. As these data reveal, rate constants in these two systems correlate very well with one another. The slope of the regression line is 0.73 ± 0.08 , which is very similar to that observed for the substituted BTCs in the same two systems.

Unlike the relatively subtle effects of substituents on the aromatic ring, substituents on the carbon center lead to more dramatic differences in reactivity of several orders of magnitude. As expected, the reactivities observed for the alkyl halide compounds are inversely related to their bond dissociation energies and one-electron reduction potentials calculated by Totten and Roberts (27) (Table S1). This indicates that, within a given system, the reactivity trend is primarily a function of the ease of bond cleavage, if no steric effects are involved.

Table S1: Reaction rate constants, 95 % confidence intervals, bond dissociation energies and one-electron reduction potentials of several R–CCl₃ compounds for reduction by Fe(0) and by Cr(II).

Compound	k_{obs} Fe(0) (s ⁻¹)	k Cr(II)^b (M ⁻¹ s ⁻¹)	BDE^c (kJ mol ⁻¹)	E₁^c (V vs. SHE)
BTC (corrected) ^a	2.68 (± 0.26)×10 ⁻³	2.19 (± 0.09)	255	
1,1,1,2-TeCA	2.66 (± 0.21)×10 ⁻⁴	4.6 (± 1.2)×10 ⁻¹	269	0.044
1,1,1-TCA	5.20 (± 0.40)×10 ⁻⁵	1.3 (± 0.3)×10 ⁻¹	291	-0.020
CCl ₃ F	1.02 (± 0.26)×10 ⁻⁵	4.9 (± 0.5)×10 ⁻²	293	-0.035
CHCl ₃	7.40 (± 1.86)×10 ⁻⁷	5.2 (± 2.1)×10 ⁻³	296	-0.145

^a The reaction rate constant for BTC was obtained in 50 % acetonitrile/50% Tris buffer (pH 7.2), whereas the other compounds were reacted in Tris buffer only (pH 7.2). For the purpose of comparability with the other rate constants, the BTC rate constant was multiplied by a factor of 7, which was the inhibitory effect caused by acetonitrile on the reactivity of iron toward 1,1,1-TCA.

^b Values taken from ref. 26.

^c Bond dissociation energies and one-electron reduction potentials for the reaction $RX \rightarrow R\cdot + X\cdot$ as calculated herein or reported in ref. 27.

Literature Cited

- (1) Castro, C. E. The role of halide in the reduction of carbonium ions by chromium(II). *J. Am. Chem. Soc.* **1961**, *83*, 3262-3264.
- (2) Kelsall, G. H.; House, C. I.; Gudyanga, F. P. Chemical and electrochemical equilibria and kinetics in aqueous Cr(III)/Cr(II) chloride solutions. *J. Electroanal. Chem.* **1988**, *244*, 179-201.
- (3) Fennelly, J. P.; Roberts, A. L. Reaction of 1,1,1-trichloroethane with zero-valent metals and bimetallic reductants. *Environ. Sci. Technol.* **1998**, *32*, 1980-1988.
- (4) Gáspár, A.; Buglyó, P. Separation and kinetic study of chromium(III) chloro complexes by capillary electrophoresis. *Chromatographia* **2000**, *51*, S-143-147.
- (5) Anet, F. A. L.; LeBlanc, E. A novel organo-chromium compound. *J. Am. Chem. Soc.* **1957**, *79*, 2649-2650.
- (6) Kochi, J. K.; Davis, D. D. Reduction of organic halides by chromium(II). Mechanisms of the formation of benzylchromium ion. *J. Am. Chem. Soc.* **1964**, *86*, 5264-5271.
- (7) Yates, K.; Stewart, R. Protonation of the carbonyl group. *Can. J. Chem.* **1959**, *37*, 664-671.
- (8) McClelland, R. A.; Coe, M. Structure-reactivity effects in the hydration of benzaldehydes. *J. Am. Chem. Soc.* **1983**, *105*, 2718-2725.
- (9) Castro, C. E.; Kray, W. C. Carbenoid intermediates from polyhalomethanes and chromium(II). The homogeneous reduction of geminal halides by chromous sulfate. *J. Am. Chem. Soc.* **1966**, *88*, 4447-4455.
- (10) Wade, R. S.; Havlin, R.; Castro, C. E. The oxidation of iron(II) porphyrins by organic molecules. *J. Am. Chem. Soc.* **1969**, *91*, 7530.
- (11) Wade, R. S.; Castro, C. E. Oxidation of iron(II) porphyrins by alkyl halides. *J. Am. Chem. Soc.* **1973**, *95*, 226-230.
- (12) Arnold, W. A.; Roberts, A. L. Pathways and kinetics of chlorinated ethylene and chlorinated acetylene reaction with Fe(0) particles. *Environ. Sci. Technol.* **2000**, *34*, 1794-1805.
- (13) Cramer, C. J. *Essentials of Computational Chemistry: Theories and Models*; Wiley: Chichester, 2002.
- (14) Becke, A. D. Density-functional thermochemistry. III. The role of exact exchange. *J. Chem. Phys.* **1993**, *98*, 5648-5652.
- (15) Stephens, P. J.; Devlin, F. J.; Ashwar, C. S.; Bak, K. L.; Taylor, P. R.; Frisch, M. J. In *Chemical Applications of Density Functional Theory*; Laird, B. B., Ross, R. B., Ziegler, T., Eds.; American Chemical Society: Washington, DC, 1996; pp 105-113.

- (16) Slater, J. C. *Quantum Theory of Molecules and Solids, Vol. 4: The Self-Consistent Field for Molecules and Solids*; McGraw-Hill: New York, 1974.
- (17) Becke, A. D. Density-functional exchange-energy approximation with correct asymptotic behavior. *Phys. Rev. A* **1988**, *38*, 3098-3111.
- (18) Lee, C.; Yang, W.; Parr, R. G. Development of the Colle-Salvetti correlation-energy formula into a functional of the electron density. *Phys. Rev. B* **1988**, *37*, 785-798.
- (19) Stephens, P. J.; Devlin, F. J.; Chabalowski, C. F.; Frisch, M. J. Ab initio calculation of vibrational absorption and circular dichroism spectra using density functional force fields. *J. Phys. Chem.* **1994**, *98*, 11623-11627.
- (20) McLean, A. D.; Chandler, G. S. Contracted Gaussian basis sets for molecular calculations. I. Second row atoms, Z=11-18. *J. Chem. Phys.* **1980**, *72*, 5639-5648.
- (21) Krishnan, R.; Binkley, J. S.; Seeger, R.; Pople, J. A. Self-consistent molecular orbital methods. XX. A basis set for correlated wave functions. *J. Chem. Phys.* **1980**, *72*, 650-654.
- (22) Clark, T.; Chandrasekhar, J.; Spitznagel, G. W.; Schleyer, P. v. R. Efficient diffuse function-augmented basis sets for anion calculations. III. The 3-21+G basis set for first-row elements, Li-F. *J. Comp. Chem.* **1983**, *4*, 294-301.
- (23) Frisch, M. J.; Pople, J. A.; Binkley, J. S. Self-consistent molecular orbital methods 25. Supplementary functions for Gaussian basis sets. *J. Chem. Phys.* **1984**, *80*, 3265-3269.
- (24) Frisch, M. J. *et al. Gaussian 03. Revision B.01*. 2003, Wallingford, CT: Gaussian, Inc.
- (25) Ebersohn, L. *Electron Transfer Reactions in Organic Chemistry*; Springer Verlag: New York, 1987.
- (26) Totten, L. A. *The Use of Model and Probe Compounds to Investigate the Mechanisms of Reductive Dehalogenation Reactions*. Ph.D. Thesis, Johns Hopkins University, Baltimore, 1999, pp 308.
- (27) Totten, L. A.; Roberts, A. L. Calculated one- and two-electron reduction potentials and related molecular descriptors for reduction of alkyl and vinyl halides in water. *Crit. Rev. Env. Sci. Tech.* **2001**, *31*, 175-221.